Desalination and Water Treatment
www.deswater.com
doi: 10.1080/19443994.2014.986204

57 (2016) 3048–3058
February

Taylor & Francis
Taylor & Francis Group

Use of activated carbon prepared from *Prosopis spicigera* L. wood (PSLW) plant material for the removal of rhodamine 6G from aqueous solution

Mahalingam Murugan[a,*], Manickam Jansi Rani[b], Perumal Subramaniam[c], Esakkiappan Subramanian[d]

[a]*Department of Chemistry, Sri K.G.S. Arts College, Srivaikuntam, Tuticorin 628 619, Tamil Nadu, India, Fax: 04630255252; email: mahalingam_murugan2004@yahoo.com*
[b]*Department of Chemistry, Govindammal Aditanar College for Women, Tiruchendur, Tuticorin 628 215, Tamil Nadu, India*
[c]*Department of Chemistry, Aditanar College of Arts and Science, Tiruchendur, Tuticorin 628 216, Tamil Nadu, India*
[d]*Department of Chemistry, Manonmaniam Sundaranar University, Tirunelveli 627012, Tamil Nadu, India*

Received 25 March 2014; Accepted 28 October 2014

ABSTRACT

The removal of rhodamine 6G dye from aqueous solution using carbon prepared from cheaply available agro-product, *Prosopis spicigera* L. wood (PSLW), was investigated. This work involves studies of physical and chemical properties of adsorbent, batch sorption experiments, and continuous run in a packed column at laboratory scale. Optimum condition for rhodamine 6G dye adsorption on PSLW carbon was determined by varying pHs, adsorbate concentrations, contact time, adsorbent dosage, and temperature. Lower solution pH favored the adsorption of Rh 6G dye. Adsorption onto the surface, surface mass transfer, and pore diffusion of dye molecules were the main process involved in the removal of Rh 6G dye. The adsorption followed Langmuir isotherm and the maximum adsorption capacity was found to be 8.86 mg/g for an initial concentration of 30 mg/L at 30°C. Thermodynamic parameters indicated that the adsorption interaction was spontaneous and exothermic in nature. The column study was explained using Thomas model.

Keywords: Adsorption; Kinetics; *Prosopis spicigera* L. wood (PSLW) carbon; Rhodamine 6G; Thomas model

1. Introduction

Dyes are indispensable in the modern sophisticated life to magnify the value of the product [1]. Colored effluents released into water bodies cause a serious health hazard to human beings and significantly affect photosynthetic activity in aquatic life [2,3]. A small quantity of dye in water is greatly noticeable and can be lethal to individuals in water. Rhodamine 6G (Rh 6G) is one such type of highly water-soluble cationic dyes. It belongs to xanthane class and is used in biological, analytical, and optical sciences [4]. It is used in textile, leather, and jute industries for dyeing cotton, silk, leather, paper, wool, and bamboo. But it makes toxic effect in the environment [5] and causes irritation to the skin, eyes, gastrointestinal tract, and respiratory tract. Therefore, the removal of Rh 6G and other coloring dyes from water is essential. Different treatment technologies such as adsorption [6], precipitation [7], ion-exchange [8],

*Corresponding author.

electrochemical oxidation [9], and biological process [10] are employed to eliminate dyes from colored waters. Among these popular techniques, adsorption on activated carbon is quite simple, household, adequate, and classic for the withdrawal of organic contaminants from wastewater [11]. Because of its high making cost, use of activated carbon is discouraging [12]. At present, therefore, significant attention is paid to identify low-cost activated carbon from economically and readily renewable existing materials of different sources [13–17]. They include banana peel [18], bagasse [19], jute fiber [20], palm-tree cobs [21], rice husks [22], nut shells [23], etc., as potential adsorbents for dye containing waters. To make effective adsorption, researches on new adsorbents are still under progress.

In this study, PSLW carbon prepared from a dry land plant material *Prosopis spicigera* L. wood (PSLW) used as firewood by the poor people, which is available all over India especially in the dry lands and deserts, is investigated for the removal of Rh 6G. This PSLW carbon is cheap, cost-effective, and widely available, but its adsorption behavior in particular toward dyes is not much studied. Hence, in the present work, we have chosen Rh 6G as a typical dye (photo-stable and not easily degraded) and investigate its adsorption on PSLW carbon. With many active sites and pores, this PSLW carbon is expected to have efficient adsorption. The results presented herein not only confirm this point but also display the interesting and typical adsorption behavior of the material.

2. Materials and methods

2.1. Materials

PSLW plant material used in the present work was collected from the dry land area of Tiruchendur in Thoothukudi district, Tamil Nadu State, India. Activated carbon was prepared from the collected plant material using the following procedure, which is adopted by the common people to produce carbon. The branches and roots of the tree were cut into pieces and pilled up on a firing hearth. Before firing, the heaped wood pieces were enclosed by fresh plantain pith and the whole mass was covered and plastered with layers of wet clay. This arrangement prevented the direct entry of air into wood pieces and hence prohibited burning of wood and of becoming ash. After 48 h of continuous firing and subsequent natural cooling, the activated carbon was obtained. The non-carbonaceous materials such as plantain pith and clay-mud were removed, and then carbon was isolated, crushed into fine powder, and sieved to 75-μm particles. The specific carbon material was stored in bottles and used as such for adsorption study after subjecting it to various physico-chemical parameters determination.

2.2. Characterization of the adsorbent

The standard procedures [24,25] were adopted to find the characteristics of activated carbon. BET method involving Quantasorb Jr surface analyzer (USA) was applied to determine the surface area and pore volume of PSLW carbon. Morphological study was carried out on Hitachi S 450 Japan, Scanning Electron Microscope (SEM). Potentiometric titration with acid/alkali was made to determine the zero point charge [26]. Fourier transform infra red (FT-IR) spectroscopy recording with Jasco FT-IR 410 spectrophotometer was performed to study the nature of the surface functional groups. Boehm titration was employed to identify the surface functional groups such as carboxyl, lactone, phenol and carbonyl, and basic and acidic sites [27,28].

2.3. Batch adsorption studies

The stock solution was prepared by dissolving one gram of dye (Rh 6G) in distilled water (1,000 mg/L) and suitably diluted to required concentrations of 20, 25, and 30 mg/L. An adsorbent dose of 2 g/L was kept constant for all the adsorption experiments. A portable digital pH meter with glass electrode model LT-120 ELICO was utilized for the measurement of pH values of the aqueous phase. The initial pH value was adjusted using 0.1 mol L^{-1} NaOH and 0.1 mol L^{-1} HCl solutions. Batch adsorption equilibrium experiments were performed using 0.1 g of PSLW carbon (particle size 75 μm) in 50 mL of dye (Rh 6G) solution and agitated in a thermostatic shaker for required time. After completion of adsorption, the adsorbent was separated by filtration and the filtrate (dye solution) was analyzed by measuring absorbance at λ_{max} of 524 nm with UV–visible spectrophotometer (ELICO BL 220 Bio double beam). The batch mode of study was performed to examine the effect of experimental parameters such as pH (1–10), initial concentrations of dye (20, 25, and 30 mg/L), contact time (5–120 min), and temperature (30–45°C). The amount of dye adsorbed per unit mass of the adsorbent (q) was calculated using Eq. (1):

$$q = \left[\left(C_i - C_f\right)V\right]/W \quad (1)$$

where q stands for the amount of dye adsorbed (mg/g), C_i , and C_f are the initial and free concentrations of dye (mg/L), V is the volume of dye solution (mL), and W is the weight of the adsorbent (g). The percent of adsorption of dye (X) was calculated using Eq. (2):

$$(X) = \left[\left(C_i - C_f\right)/C_i\right] \times 100 \quad (2)$$

2.4. Column study

In column study, 5 g of PSLW carbon (particle size 75 μm) was first washed with distilled water to remove carbon fines and then packed evenly in a glass column (1.5 cm diameter and 65 cm height) by tapping to reduce air voids in the carbon bed for a bed height of 7.5 cm. Synthetic (Rh 6G) dye solution of concentration 25 mg/L of 2.5 L was drawn into the column at a rate of 1 mL/min from a separatory funnel fixed at a height of 1 m. The column was operated continuously with dye solution, and the height was maintained constant throughout the operation to maintain the flow accurately. Effluents were collected at regular intervals of time and analyzed. The column flow was terminated when the ratio of the effluent to influent dye (Rh 6G) concentration reached a value of 0.8. After column exhaustion, the adsorbed Rh 6G was eluted with 500 mL of ethanol.

3. Results and discussion

3.1. Characterization of the adsorbent

The physico-chemical characteristics of PSLW are given in Table 1. From the BET method, the surface area and pore volume of PSLW carbon are found to be 120.91 m^2/g and 0.97 cm^3, respectively. The pH_{pzc} value of PSLW carbon is 6.98. The scanning electron micrograph of PSLW carbon (Fig. 1(a)) shows fibrous surface morphology with a fully developed porous structure. Cavities and irregular pores are traced on the external surface of the activated carbon. The FT-IR spectrum of free PSLW carbon (Fig. 2(a)) shows a broad band at 3,317 cm^{-1} attributable to –OH stretch from carboxylic groups (–COOH and –OH) [28], while the weak band at 1,637 cm^{-1} may be related to –C=O stretch from carboxylic group, and the peak at about 1,400 cm^{-1} may be due to stretching vibration of lactone =C–O, –CH=, and $–CH_2$ groups [29]. Boehm titration (acid/base neutralization experiments) gives the quantitative estimation of surface functional groups such as carboxyl, lactones, phenols, acidic, and basic sites and their values are 3.44, 0.145, 0.915, 3.5, and 14.5 meq/g, respectively. The PSLW carbon has more basic sites than acidic sites. This type of carbon material has been reported in the literature [30].

Table 1
Characteristics of the adsorbent PSLW carbon (75 μm)

Parameter	Value
Bulk density (g/cc)	0.222
Particle density (g/cc)	0.181
Moisture content % (w/w)	12.0
Pore space volume (mL)	5.50
pH	6.50
pH_{pzc}	6.98
Surface area (m^2/g)	120.9
Pore volume (cm^3)	0.970
Carboxyl group (meq/g)	3.44
Lactones (meq/g)	0.145
Phenolic (meq/g)	0.915
Base (meq/g)	14.5

3.2. Effect of pH

pH is one of the significant parameters which influences the adsorption process. Fig. 3 shows the effect of pH in the range of 1.0–10.0. From the figure, it is noted that the maximum adsorption (i.e. 88%) of Rh 6G dye is achieved at pH 4.0. It was believed that at lower pH, more adsorption of dye is due to strong electrostatic force of attraction between the basic sites of PSLW carbon and cationic dye [31,32]. But electrostatic interaction is minimum, contradictory to the expectation that at pH lower than pH_{pzc}, the dye adsorption is found to be maximum at pH 4.0. The quiet unexpected observation is explicable as follows. Although PSLW carbon has more basic sites, their contribution through electrostatic interaction is minimum. This conclusion is emerged from the observation of desorption study. With ethanol, maximum dye desorption (60.5%) and with sodium hydroxide minimum dye desorption (32.45%) have been observed. The lowest desorption efficiency of sodium hydroxide clearly suggests the less importance of electrostatic interaction in dye adsorption. Therefore, other types of interaction particularly hydrogen bonding of –NH and ester group of dye with –OH, –COOH, and lactone groups of PSLW carbon; hydrophobic interaction between phenyl rings of dye and PSLW carbon phase etc., also play major role in dye adsorption. This is evident from the IR spectrum of Rh 6G-loaded PSLW carbon (Fig. 2(b)). In IR spectrum of Rh 6G-loaded PSLW carbon, the peak corresponding to hydroxyl group remains unaffected and the peak intensity at 1,637 cm^{-1} is decreased. A strong evidence in favor of

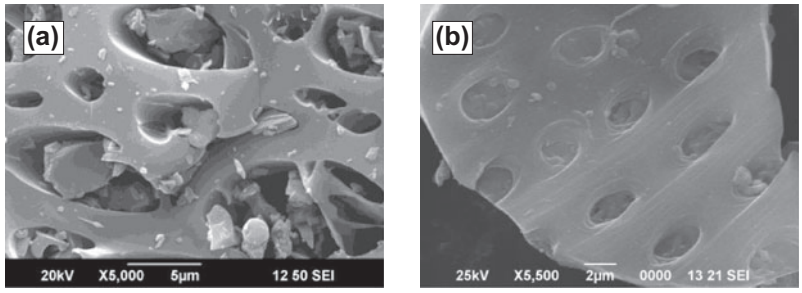

Fig. 1. SEM images of (a) free and (b) Rh 6G-loaded PSLW carbon.

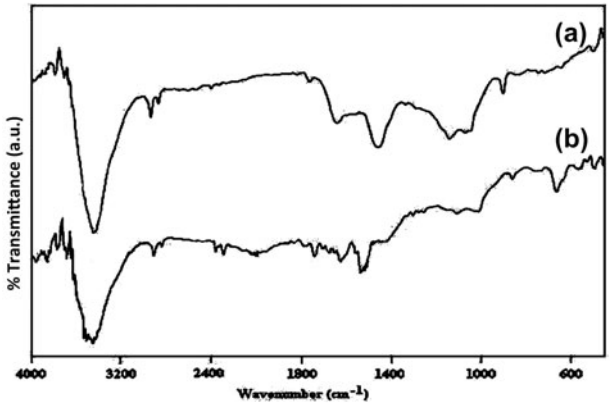

Fig. 2. FT-IR spectra of (a) free and (b) dye Rh 6G-loaded PSLW carbon.

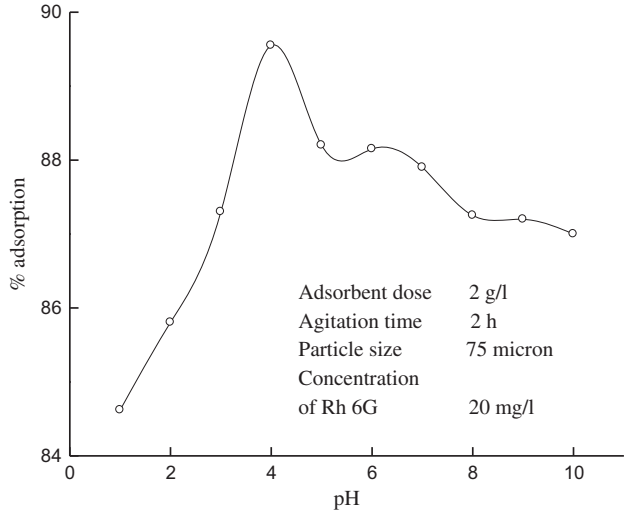

Fig. 3. Effect of pH on adsorption of Rh 6G on PSLW carbon.

hydrogen bonding from dye to carbon occurs in the observation that the peak at about 1,400 cm^{-1} due to lactone groups in free PSLW carbon (Fig. 2(b)) gets shifted to higher wave number side (~1,450 cm^{-1}). All these IR changes on dye adsorption show the involvement of surface functional groups' (electrophilic, hydrogen bonding, hydrophobic, etc.) interaction with Rh 6G dye. In addition, a new peak in the region 600–800 cm^{-1} appears due to the C-Rh 6G stretching vibration. Further SEM analysis after adsorption (Fig. 1(b)) shows the presence of spherical particles on the surface of Rh 6G-loaded PSLW carbon and this indicates the adsorption of dye molecules on the surface of PSLW carbon.

3.3. Effect of contact time, initial dye concentration, and adsorbent dosage

The adsorption capacity of PSLW carbon for Rh 6G dye was investigated as a function of contact time at different initial concentrations of the dye (20, 25, 30 mg/L). From Fig. 4, it is found that the equilibrium uptake of dye increases with increase in contact time and the equilibrium is reached at 60 min. After reaching the state of equilibrium, there is no significant increase in the adsorbed amount. The maximum adsorption capacity of Rh 6G dye at three different initial dye concentrations of 20, 25, and 30 mg/L are found to be 9.75, 10.87, and 11.97 mg/g, respectively.

Adsorbent dosage study (Fig. 5) shows that an increase in adsorbent dose increases the removal percentage of dye. It means that increasing the adsorbent dose increases the number of adsorption active sites which in turn increases the removal of higher amount of dye [33]. According to Fig. 5, the increase in the adsorbent amount may lead to aggregate the adsorption sites, resulting in decrease in the total available surface area of adsorbent; hence, the adsorption amount decreases at higher adsorbent amount.

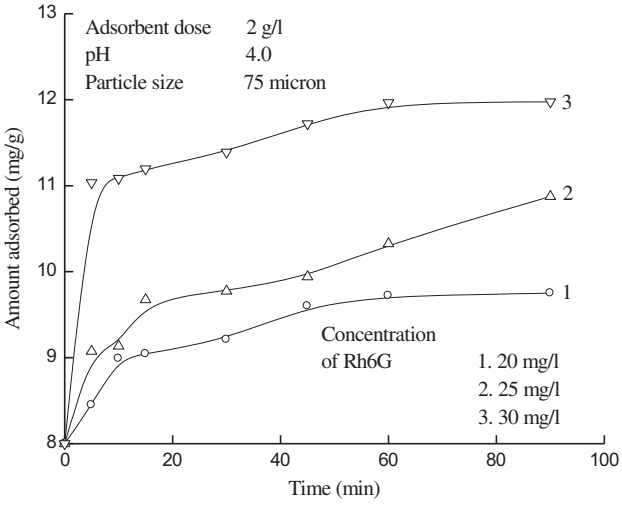

Fig. 4. Effect of contact time and initial concentration on the adsorption of Rh 6G.

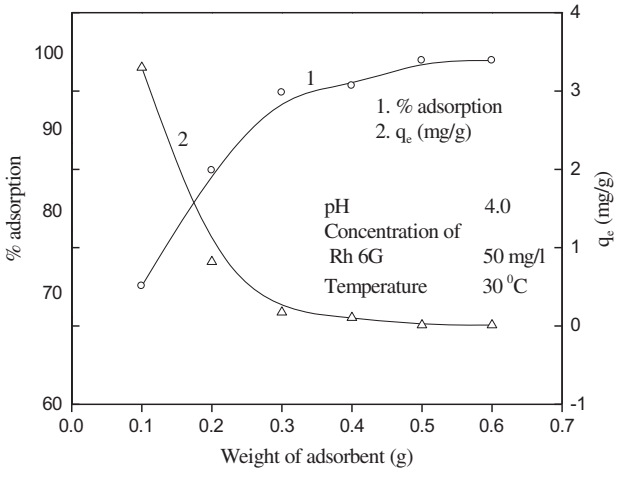

Fig. 5. Effect of adsorbent dose for Rh 6G adsorption.

3.4. Effect of temperature

Temperature plays an important role in determining the adsorption capacity. The effects of the temperature (30–45°C) on adsorption are shown in Fig. 6. It depicts that the adsorption capacity of PSLW carbon decreases with the increase in temperature [34], thereby indicating that the adsorption of dye onto PSLW carbon is an exothermic process.

3.5. Thermodynamic behavior

The thermodynamic parameters determining the nature of thermodynamic feasibility of the adsorption process such as standard free energy (ΔG°), standard

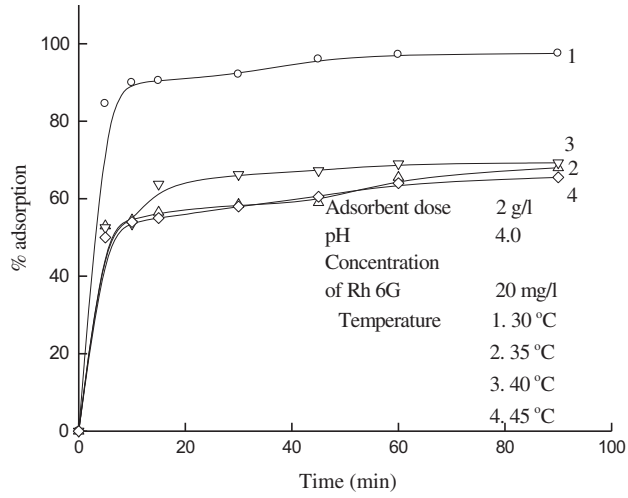

Fig. 6. Effect of temperature on adsorption of Rh 6G.

enthalpy (ΔH°), and standard entropy (ΔS^{o}) are determined using Eqs. (3)–(5):

$$\Delta G^{\circ} = -RT \ln K \tag{3}$$

$$\log K = \Delta S^{\circ}/2.303RT - \Delta H^{\circ}/2.303RT \tag{4}$$

$$\Delta G^{\circ} = \Delta H^{\circ} - T\Delta S^{\circ} \tag{5}$$

where R, T, and K represent the universal gas constant (8.314 J/mo1/K), temperature in Kelvin, and the equilibrium constant, respectively. The values of thermodynamic parameters (Table 2) provide information for understanding the nature of adsorption process. The ΔG° values are found to be negative that indicate the adsorption process is spontaneous in nature. The low negative value of ΔH° denotes that the nature of adsorption process is exothermic. This is also supported by the decrease in value of uptake capacity of the adsorbent with the increase in temperature (Fig. 6). The positive value of ΔS° suggests good affinity of the dye toward adsorbent. Thus, thermodynamic parameters indicate that the adsorption process is spontaneous and exothermic in nature [34].

3.6. Isotherm analysis

The adsorption data are analyzed with two well-known adsorption isotherm models namely Langmuir [35] and Freundlich [36], which are expressed by Eqs. (6) and (7), respectively.

Table 2
Thermodynamic parameters for the adsorption of Rh 6G on PSLW carbon

Temperature (°C)	$-\Delta G^{\circ}$ (kJ/mol)	$-\Delta H^{\circ}$ (kJ/mol)	$-\Delta S^{\circ}$ (J/mol K)
30	7.06	35.91	0.166
35	15.13		
40	16.65		
45	16.84		

$$C_f/q = 1/Q_o b + C_f/Q_o \quad (6)$$

$$\log q = \log K_f + 1/n \log C_f \quad (7)$$

where q stands for amount of Rh 6G dye adsorbed (mg/g), C_f is the concentration of the free adsorbate (mg/L) at equilibrium, Q_o is the Langmuir constant representing the maximum monolayer adsorption capacity, b is the Langmuir constant related to energy of adsorption, and K_f and $1/n$ are Freundlich constants related to adsorption capacity and adsorption intensity, respectively. The experimental data fit well to the Langmuir model but not to Freundlich model. This is evident from the linear plots of C_f/q against C_f in Langmuir model for the adsorption of Rh 6G dye on PSLW carbon (Fig. 7) but for Freundlich model the plots are not linear as per eqn. (7) (figure not shown). Q_o and b can be determined from the slope and intercept of the linear plots in Fig. 7 and are given in Table 3. All these facts prove that Rh 6G dye is adsorbed as monolayer coverage on the surface of the adsorbent. Further the dimensionless separation factor (R_L) is calculated [37] using Eq. (8):

$$R_L = 1/1 + bC_o \quad (8)$$

The observed R_L values lie between zero and one (Table 3), which establish the fact that the adsorption process is favorable under the studied conditions.

3.7. Adsorption kinetics

Adsorption kinetics provides the knowledge on the adsorption mechanism of adsorbate onto an adsorbent. The kinetics of Rh 6G dye adsorption on PSLW carbon was examined with pseudo-first-order [38,39] and pseudo-second-order [40,41] models which are represented by Eqs. (9) and (10), respectively:

$$\log (q_e - q) = \log q_e - (K_1 t/2.303) \quad (9)$$

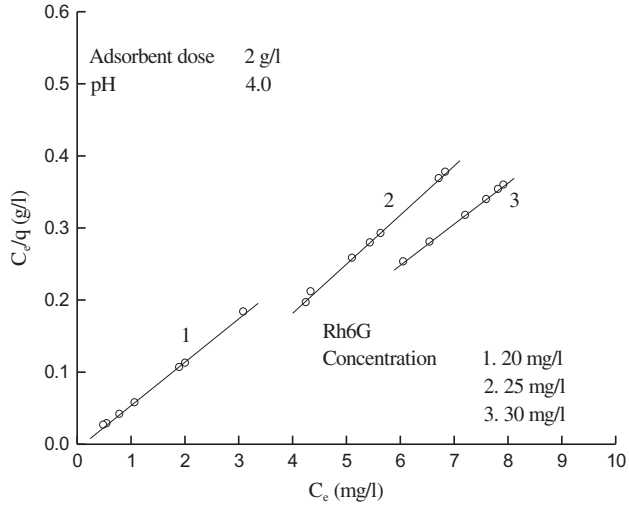

Fig. 7. Langmuir isotherm for Rh 6G at different concentrations.

$$t/q_t = 1/K_2 q_e^2 + t/q_e \quad (10)$$

where q_e and q_t are the amount of dye adsorbed (mg/g) at equilibrium and at time "t" (min), respectively. K_1 (L/min) and K_2 (g/mg/min) are the adsorption rate constants. For the studied initial concentrations and temperatures, the rate constants (K_1 and K_2) and theoretical equilibrium adsorption capacities, q_e(cal), calculated from the slope and intercept of the linear plots of the pseudo-first-order and pseudo-second-order kinetic models (Fig. 8), and the co-efficient of linear correlation (R^2) are given in Table 4.

An analysis of values in Table 4, particularly the examination of agreement between q_e (exp) and q_e (cal), and the closeness of R^2 values toward unity at different initial concentrations and temperatures for both pseudo-first-order and pseudo-second-order models clearly reveals that pseudo-second-order

Table 3
Langmuir constants and equilibrium parameters

Concentration (mg/L)	Q_o (mg/g)	b (L/mg)	R_L	R^2
20	8.27	8.608	0.006	0.999
25	7.46	0.796	0.048	0.999
30	8.86	0.639	0.050	0.999

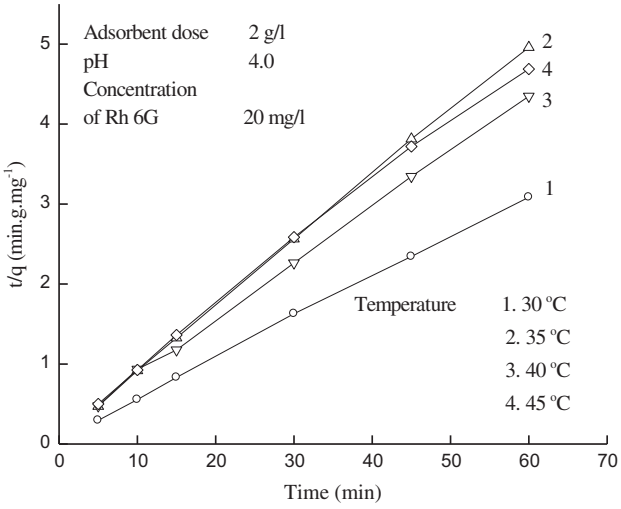

Fig. 8. Pseudo-second order plots at different temperatures.

model fits better to the data. Therefore, it is inferable that the adsorption of Rh 6G dye on PSLW carbon can be well described by Lagergren second-order kinetics.

3.8. Intra-particle diffusion

Fig. 9 depicts the plots of amount of adsorption vs. $t^{1/2}$. They are parabolic yet linear for some contact times at the initial stage, and moreover, they do not pass through origin [42]. The intra-particle diffusion constant, K_i given by the slope of the linear portion of the plots is determined and reported in Table 4. This pattern obviously indicates that the dye molecules slowly enter into the interior of the PSLW carbon particles through the pores step on the surface and get entrapped in the interior.

3.9. Mass transfer study

The external mass transfer was studied using the mathematical mass transfer model proposed by McKay et al. [43], which is expressed in Eq. (11):

$$\ln(C_t/C_o - 1/1 + mk) = [(1 + mk/mk)\beta_L S_s)]t + (mk/1 + mk) \quad (11)$$

where C_o (mg/L) is the initial adsorbate concentration; C_t is the adsorbate concentration after time t; m (g/L) is the mass of adsorbent per unit volume of particle free adsorbate solution; k (L/g) is the Langmuir constant obtained by multiplying adsorption capacity, Q_o, and adsorption energy, b; β_L (cm/s) is the mass transfer coefficient; and S_s (cm^{-1}) is the outer surface area of the adsorbent per unit volume of particle free slurry. The values of "m" and S_s were calculated using the relations (12) and (13):

$$m = W/v \quad (12)$$

$$S_s = 6m/(1 - \varepsilon_p)d_p\rho_p \quad (13)$$

where W (g) is the weight of absorbent; "v" (L) is the volume of particle free adsorbate solution; d_p is the particle diameter (cm); ρ_p (g/cm^3) is the density of adsorbent; and ε_p is the porosity of adsorbent particle. The $\ln[(C_t/C_o - 1/1 + mk)]$ vs. time plots were made. They exhibit a linear behavior indicating the rapid transport of dye molecules from bulk to solid phase. The values of mass transfer coefficients obtained from the slope and intercept are entered in Table 5. The mass transfer coefficients decrease with increase in temperature.

3.10. Column study

Column adsorption process is vital to industrial process for wastewater treatment. The observed data fit to the linearized form of the Thomas model [44,45] and are given in Eq. (14):

$$\log (C_o/C_e - 1) = Kq_oM/Q - KC_oV/Q \quad (14)$$

Table 4
Comparison of pseudo-first order and pseudo-second order model parameters

Temperature (°C)	q_e exp (mg/g)	Pseudo first order $K_1 \times 10^2$ (min^{-1})	Pseudo first order q_e cal (mg/g)	Pseudo first order R^2	Pseudo second order $K_2 \times 10^2$ (g/mg/min)	Pseudo second order q_e cal (mg/g)	Pseudo second order R^2	Intra-particle diffusion constant Ki ($mg/g/min^{1/2}$)
30	9.75	6.22	1.91	0.96	7.8	9.88	0.99	0.0999
35	6.80	1.27	1.50	0.89	4.18	6.77	0.99	0.1727
40	6.92	7.00	2.45	0.97	6.4	7.06	0.99	0.1837
45	6.9	3.70	1.92	0.97	4.8	6.70	0.99	0.1899

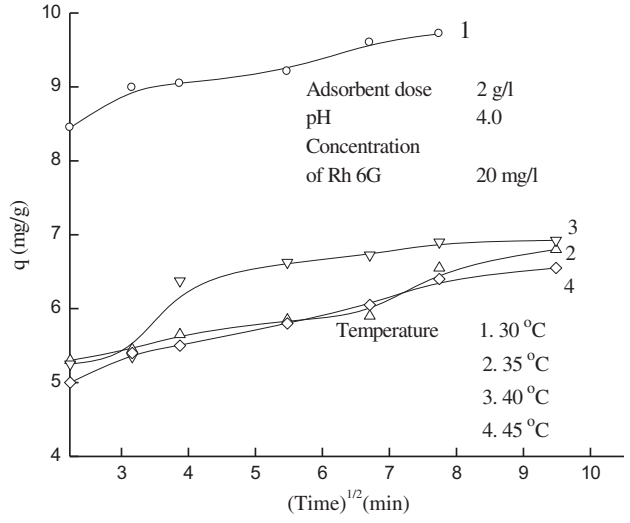

Fig. 9. Plots of intra particle diffusion at different temperatures.

where C_o and C_e are the influent and effluent Rh 6G concentrations (mg/L), respectively. While K stands for the Thomas rate constant (mL/min/mg), q_o is the maximum solid phase concentration of solute (mg/g), M is the mass of the adsorbent (g), and V is the throughput volume (mL/min). Fig. 10 clearly displays the breakthrough curve of the adsorption of Rh 6G dye on PSLW carbon (particle size 75 μm). Concentrations of effluent dye are found to be zero for first 90 bed volumes, 90% of dyes is retained for next 20 bed volumes, and 80% for another 10 bed volumes. After 120 bed volumes, the retention of Rh 6G dye by the column gradually declines as the bed volume increases. The values of K and q_o are computed from the slope and intercept of the linear plot of log $(C_o/C_e - 1)$ vs. V, and they are found as 5.311×10^{-2} (mL/min/mg) and 9.11 (mg/g). When the PSLW carbon was saturated with Rh 6G dye, the latter was eluted with 500 mL of ethanol. The desorption study shows the reusability of the adsorbent, and hence, it is highly economical. Thus, column analysis using PSLW carbon can be applied to the industrial process for the removal of dyes from aqueous solution.

Table 5
Mass transfer coefficients at different temperatures

Temperature (°C)	Mass transfer coefficient (cm/s) × 10^3
35	1.228
40	1.549
45	1.525

3.11. Desorption study

Desorption experiment was carried out by placing 0.1 g of Rh 6G-loaded PSLW carbon in 50 mL of ethanol, 0.1 N HCl, chloroform, and 0.1 N NaOH at 30°C. The percent desorption was 60.5, 46.5, 55.7, and 33.5, respectively, for ethanol, HCl, chloroform, and NaOH.

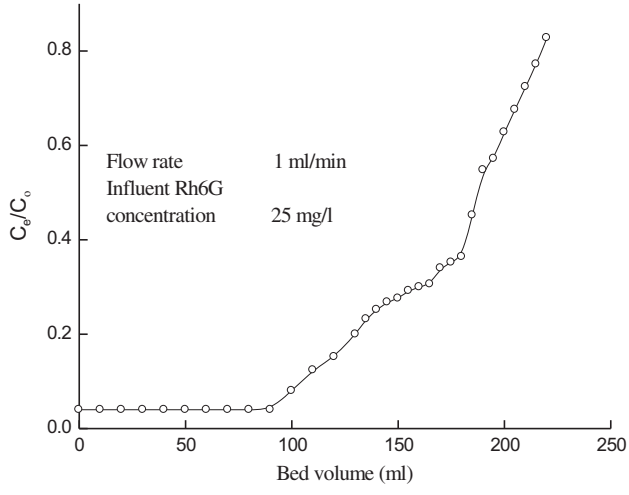

Fig. 10. Breakthrough curves for adsorption of Rh 6G on PSLW carbon.

Table 6
Comparison of PSLW carbon with different adsorbents

S. No.	Adsorbent	Adsorption capacity, q (mg/g)	Reference
1	*Sterculia Quadrifida* Shell Waste activated carbon	104.26	[46]
2	*Jatropha* husk carbon	50	[47]
3	bamboo seed activated carbon	1.855	[48]
4	Cocoa shell activated carbon	41.67	[49]
5	*Acacia nilotica* leaves carbon	37	[50]
6	Coconut shell carbon	2.33	[51]
7	*Thespusia populinia* bark carbon	60.83	[52]
8	E*rythrina indica* bark carbon	333.33	[53]
9	PSLW carbon	8.86	Present study

3.12. Comparison of PSLW carbon with different adsorbents

The adsorption capacity of the prepared PSLW activated carbon for Rh6G adsorption is compared with the previously used adsorbents in the literature and is given in Table 6. From the table, it is observed that the PSLW carbon has a comparable adsorption capacity with other adsorbents.

4. Conclusions

This study investigates the suitability of PSLW carbon as a potential adsorbent for the effective removal of Rh 6G dye from aqueous solution using batch and column methods. The maximum adsorption of Rh 6G dye is achieved at pH 4.0. The maximum adsorption capacity of Rh 6G dye is found to be 9.75, 10.87, and 11.97 mg/g, for initial concentrations of 20, 25, and 30 mg/L, respectively. Equilibrium adsorption data fit well to the Langmuir isotherm model. From the thermodynamic studies, the adsorption of Rh 6G dye on PSLW carbon is spontaneous, exothermic, and thermodynamically favorable at low temperature. The kinetic data fit well to the pseudo-second-order rate equations with multi-step intra-particle diffusion. Column adsorption data are effectively described by Thomas model, and the maximum adsorption capacity of PSLW activated carbon is found to be 9.11 mg/g in column mode. Thus, the study concludes that the PSLW carbon seems to be an efficient, cost-effective, and unconventional adsorbent for the removal of Rh 6G dye from aqueous solutions.

References

[1] M. Arulkumar, P. Sathishkumar, T. Palvannan, Optimization of Orange G dye adsorption by activated carbon of *Thespesia populnea* pods using response surface methodology, J. Hazard. Mater. 186 (2011) 827–834.
[2] H. Zolliger, Color Chemistry-Synthesis, Properties and Applications of Organic Dyes and Pigments, VCH Publishers, New York, NY, 1987, p. 92.
[3] F. Derbyshire, M. Jagtoyen, R. Andrews, A. Rao, I. Martin Gullon, E. Grulke, C*arbon* Materials in Environmental Applications, in: L.R. Radovic (Ed.), Chemistry and Physics of Carbon, vol. 27, Marcel Dekker, New York, NY, 2001, pp. 1–66.
[4] R. Sumanta, I. Ivan, H.Q. Nurul, N.B. Sati, Photostability of rhodamine–B/montmorillonite nanopigments in polypropylene matrix, Appl. Clay Sci. 42 (2009) 661–666.
[5] M. Slimane, H. Oualid, S. Fethi, C. Mahdi, P. Chrisitian, Influence of bicarbonate and carbonate ions on sonochemical degradation of rhodamine B in aqueous phase, J. Hazard. Mater. 175 (2010) 593–599.
[6] S. Chen, J. Zhang, C. Zhang, Q. Yue, Y. Li, C. Li, Equilibrium and kinetic studies of methyl orange and methyl violet adsorption on activated carbon derived from *Phragmites australis*, Desalination 252 (2010) 149–156.
[7] A.K. Verma, R.R. Dash, P. Bhunia, A review on chemical coagulation/flocculation technologies for removal of colour from textile wastewaters, J. Environ. Manage. 93 (2012) 154–168.
[8] O. Ozdemir, B. Armagan, M. Turan, M.S. Çelik, Comparison of the adsorption characteristics of azo-reactive dyes on mezoporous minerals, Dyes Pigments. 62 (2004) 49–60.
[9] J.H.B. Rocha, N.S. Fernandes, K.R. Souza, D.R.D. Silva, M.A. Quoroz, C.A.M. Huitle, Electrochemical decolourization process of textile dye in the presence of NaCl at boron doped diamond electrode, Sustain. Environ. Res. 21 (2011) 291–298.
[10] B.E. Barragán, C. Costa, M. Carmen Márquez, Biodegration of azo dyes by bacteria inoculated on solid media, Dyes Pigments. 75 (2007) 73–81.
[11] E. Eren, B. Afsin, Removal of basic dye using raw and acid activated bentonite samples, J. Hazard. Mater. 166 (2009) 830–835.
[12] T. Ibrahim, B.L. Moctar, K. Tomkouani, D.B. Gbandi, D.K. Victor, N. Phinthe, Kinetics of the adsorption of anionic and cationic dyes in aqueous solution by low-cost activated carbons prepared from sea cake and cotton cake, Am. Chem. Sci. J. 4 (2014) 38–57.
[13] Y. Haldorai, J.J. Shim, An efficient removal of methyl orange dye from aqueous solution by adsorption onto

chitosan/MgO composite: A novel reusable adsorbent, Appl. Surf. Sci. 292 (2014) 447–453.
[14] M. Rafatullah, O. Sulaiman, R. Hashim, A. Ahmad, Adsorption of methylene blue on low-cost adsorbents: A review, J. Hazard. Mater. 177 (2010) 70–80.
[15] Z. Ioannou, J. Simitzis, Adsorption of methylene blue dye onto activated carbons based on agricultural by-products: equilibrium and kinetic studies, Water Sci. Technol. 67 (2013) 1688–1694.
[16] S. Chen, J. Zhang, C. Zhang, Q. Yue, Y. Li, C. Li, Equilibrium and kinetic studies of methyl orange and methyl violet adsorption on activated carbon derived from *Phragmites australis*, Desalination 252 (2010) 149–156.
[17] S. Ruchi, B. Mahendra, Sumit, Magan Lal, G. Vikal, Removal of Cr(VI) by *Prosopis cineraria* leaf powder- A green remediation, Indian J. Chem. Technol. 20 (2013) 312–316.
[18] G. Annadurai, R.S. Juang, D.J. Lee, Use of cellulose-based wastes for adsorption of dyes from aqueous solutions, J. Hazard. Mater. 92 (2002) 263–274.
[19] P. Sharma, H. Kaur, Sugarcane bagasse for the removal of erythrosin B and methylene blue from aqueous waste, Appl. Water Sci. 1 (2011) 135–145.
[20] S. Senthilkumaar, P.R. Varadarajan, K. Porkodi, C.V. Subbhuraam, Adsorption of methylene blue onto jute fiber carbon: Kinetics and equilibrium studies, J. Colloid Interface Sci. 284 (2005) 78–82.
[21] J. Avom, J.K. Mbadcam, C. Noubactep, P. Germain, Adsorption of methylene blue from an aqueous solution on to activated carbons from palm-tree cobs, Carbon 35 (1997) 365–369.
[22] V.K. Verma, A.K. Mishra, Kinetic and isotherm modeling of adsorption of dyes onto rice husk carbon, Global NEST J. 12 (2010) 190–196.
[23] H.B. Senturk, D. Ozdes, C. Duran, Biosorption of Rhodamine 6G from aqueous solutions onto almond shell, (*Prunus dulcis*) as a low cost biosorbent, Desalination 252 (2010) 81–87.
[24] APHA, Standard methods for the examination of water and waste water, seventeenth ed., American Water Works Association, New York, NY, 1989.
[25] BIS, Activated Carbon Powdered and Granular Methods of Sampling and Tests, Bureau of Indian Standards, New Delhi, 1S:877-0989, 1989.
[26] J.A. Schwarz, C.T. Driscoll, A.K. Bhanot, The zero point of charge of silica—Alumina oxide suspensions, J. Colloid Interface Sci. 97 (1984) 55–61.
[27] H.P. Boehm, Some aspects of the surface chemistry of carbon blacks and other carbons, Carbon 32 (1994) 759–769.
[28] M. Cheng Shih, Kinetics of the batch adsorption of methylene blue from aqueous solutions onto rice husk: Effect of acid-modified process and dye concentration, Desalin. Water Treat. 37 (2012) 200–214.
[29] Q. Shi, J. Zhang, C. Zhang, C. Li, B. Zhang, W. Hu, J. Xu, R. Zhao, Preparation of activated carbon from cattail and its application for dyes removal, J. Environ. Sci. 22 (2010) 91–97.
[30] C. Lu, C. Liu, Removal of nickel(II) from aqueous solution by carbon nanotubes, J. Chem. Technol. Biotechnol. 81 (2006) 1932–1940.
[31] M.F. Hou, C.X. Ma, W.D. Zhang, X.Y. Tang, Y.N. Fan, H.F. Wan, Removal of rhodamine B using iron-pillared bentonite, J. Hazard Mater. 186 (2011) 1118–1123.
[32] X. Xiangheng, H. Xisheng, Z. Yonghong, Adsorptive properties of acid-heat activated rectorite for Rhodamine B removal: Equilibrium, kinetic studies, Desalin. Water Treat. 37 (2012) 259–267.
[33] I.D. Mall, N.K. Agarwal, V.C. Srivastava, Adsorptive removal of Auramine-O: Kinetic and equilibrium study, J. Hazard Mater. 143 (2007) 386–395.
[34] M.F. Elkady, A.M. Ibrahim, M.M. Abd El-Latif, Assessment of the adsorption kinetics, equilibrium and thermodynamic for the potential removal of reactive red dye using eggshell biocomposite beads, Desalination 278 (2011) 412–423.
[35] I. Langmuir, The constitution and fundamental properties of solids and liquids, J. Am. Chem. Soc. 38 (1916) 2221–2295.
[36] H.M.F. Freundlich, Uber die adsorption in losungen, Z. Phys. Chem. 57(A) (1906) 384–470.
[37] T.W. Weber Jr, R.K. Chakravorti, Pore and solid diffusion models for fixed-bed adsorbers, J. Am. Inst. Chem. Eng. 20 (1974) 228–238.
[38] S. Lagergren, K. Svenska, About the theory of so-called adsorption of soluble Substances, K. Svenska Ventenskapsakad. Handl. 24 (1898) 1–39.
[39] Y.S. Ho, Citation review of lagergren kinetic rate equation on adsorption reactions, Scientometrics 59 (2004) 171–177.
[40] Y.S. Ho, G.M. McKay, Pseudo-second-order model for sorption processes, Process Biochem. 34 (1999) 451–465.
[41] X.Y. Yang, S. Robert Otto, B. Al-Duri, Concentration-dependent surface diffusivity model (CDSDM): Numerical development and application, J. Chem. Eng. 94 (2003) 199–209.
[42] D.S. Sun, X.D. Zhang, Y.D. Wu, X. Liu, Adsorption of anionic dyes from aqueous solution on fly ash, J. Hazard. Mater. 181 (2010) 335–342.
[43] G. McKay, M.S. Otterburn, A.G. Sweeney, Surface mass transfer processes during colour removal from effluent using silica, Water Res. 15 (1981) 327–331.
[44] H.C. Thomas, Chromatography: A Problem in kinetics, Ann. NY Acad. Sci. 49 (1948) 161–182.
[45] T.D. Reynolds, P.A. Richards, Unit operations and processes in Environmental Engineering, PWS, Boston, MA, 1996, P. 142.
[46] S. Karthikeyan, P. Shanthi, A. Saravanan, K. Saranya, Sorption of basic dye (Rhodamine B) by nano porous activated carbon from *Sterculia Quadrifida* shell waste, J. Environ. Nanotechnol. 3 (2014) 88–100.
[47] K. Karthick, C. Dinesh, C. Namasivayam, Utilization of $ZnCl_2$ activated *Jatropha* husk carbon for the removal of reactive and basic dyes: Adsorption equilibrium and kinetic studies, Sustain. Environ. Res. 24 (2014) 139–148.
[48] L.H. Khdeem, Use of charcoal derived from bamboo seed for adsorption of dyes, Inter. J. Current Res. 5 (2013) 1307–1313.
[49] C. Theivarasu, S. Mylsamy, Equilibrium and Kinetic adsorption studies of Rhodamine-B from aqueous solutions using cocoa *(Theobroma cacao)* shell as a new adsorbent, Inter. J. Eng. Sci. Technol. 2 (2010) 6284–6292.
[50] A.L. Prasad, T. Santhi, Adsorption of hazardous cationic dyes from aqueous solution onto *Acacia nilotica* leaves as an eco friendly adsorbent, Sustain. Environ. Res. 22 (2012) 113–122.

[51] K. Balasubramani, N. Sivarajasekar, Adsorption studies of organic pollutants onto activated carbon, Inter. J. Innova. Res. Sci. Eng. Technol. 3 (2014) 10575–10581.
[52] M. Hema, S. Arivoli, Rhodamine B adsorption by activated carbon: Kinetics and equilibrium studies, Indian J. Chem. Technol. 16 (2009) 38–45.
[53] V. Roopa, K. Ramesh, A. Rajappa, V. Nandhakumar, Equilibrium and isotherm studies on the adsorption of rhodamine B onto activated carbon prepared from bark of E*rythrina indica*, Int. J. Curr. Res. Chem. Pharma. Sci. 1 (2014) 23–29.